Research Article **Open Access**

Aslak Tveito*, Mary M. Maleckar, and Glenn T. Lines

Computing optimal properties of drugs using mathematical models of single channel dynamics

https://doi.org/10.1515/cmb-2018-0004
Received June 28, 2018; accepted October 6, 2018

Abstract: Single channel dynamics can be modeled using stochastic differential equations, and the dynamics of the state of the channel (e.g. open, closed, inactivated) can be represented using Markov models. Such models can also be used to represent the effect of mutations as well as the effect of drugs used to alleviate deleterious effects of mutations. Based on the Markov model and the stochastic models of the single channel, it is possible to derive deterministic partial differential equations (PDEs) giving the probability density functions (PDFs) of the states of the Markov model. In this study, we have analyzed PDEs modeling wild type (WT) channels, mutant channels (MT) and mutant channels for which a drug has been applied (MTD). Our aim is to show that it is possible to optimize the parameters of a given drug such that the solution of the MTD model is very close to that of the WT: the mutation's effect is, theoretically, reduced significantly. We will present the mathematical framework underpinning this methodology and apply it to several examples. In particular, we will show that it is possible to use the method to, theoretically, improve the properties of some well-known existing drugs.

1 Introduction

Fluxes through single ion channels serve functions as diverse as volumetric homeostasis of cells to the excitability of their membranes, and are thus of paramount importance in biology[1]. The ability to measure this flow represented a breakthrough leading to improved mechanistic understanding of excitable biological membranes and their dynamics [2–5]. Furthermore, availability of measurements from single ion channels furnished dynamic data to inform developing mathematical models. Theoretically, single channel dynamics can conveniently be represented using Markov models. While initial models of this type, which may serve to supplement sparse data and provide a theoretical framework for compact representation and development of testable hypotheses, were developed by Colquhoun and Hawkes [6, 7], more recently, the inverse problem of determining the parameters of a Markov model based on single channel data have been addressed by several groups, see e.g. [8–15].

Genetic mutations to proteins composing single ion channels can significantly alter their function, often leading to severe dysfunction, i.e. disposition to cardiac arrhythmia. As noted above, mathematical models may serve as a useful testbed by which to investigate aberrant ion channel function and to suggest a theoretical pathway for exploring treatment. Conveniently, the effects of a mutation on an ion channel can be efficiently expressed in terms of changes to a Markov model representing wild type channels; e.g. [16–20].

***Corresponding Author: Aslak Tveito:** Simula Research Laboratory, Norway
and Department of Informatics, The University of Oslo, Norway, E-mail: aslak@simula.no
Mary M. Maleckar: Allen Institute for Cell Science, Seattle, WA, USA
Glenn T. Lines: Simula Research Laboratory, Norway

Mutation-induced dysfunction can often be relieved by pharmacological intervention, and the effect of drugs on single channel dynamics can also be studied using Markov models [21–26].

Since Markov models are such a versatile tool for understanding single ion channel dynamics (wild-type, as well as with perturbation via mutation and/or drugs), it is important be able to analyze these models efficiently and accurately. A major step in this direction is the development of deterministic partial differential equations which provide the probability density functions of the stochastic variables representing the states of the Markov model; see e.g. [27–30].

In the present paper, we review the development of mathematical methods for analyzing Markov models which characterize the effects of drugs on single channel dynamics. We will explain the use of stochastic models to represent single channel dynamics, and outline how Markov models are used to represent the state of ion channels. We introduce master equations associated with the Markov models and derive formulas for the equilibrium solutions of these master equations. Deterministic partial differential equations (PDE) describing the probability density functions (PDF) of the states of the Markov model are introduced, and both numerical and analytical techniques are used to study these equations. We use PDE to show how PDF depend on the drug properties, and use these to derive optimal properties of the drugs with respect to normalizing ion channel function in regard to wild type models.

As an exemplar, we apply the mathematical models to study the release of calcium ions from internal storage structures (the sarcoplasmic reticulum, SR) of cardiac muscle cells, and to study effects of mutations on the sodium channel located at the cardiac muscle cell membrane. In both cases, we compute optimal properties of theoretical drugs represented in terms of Markov models. In some cases, we show that we can analytically derive a theoretical drug that completely rectifies the effect of a mutation; in other cases, we need to run numerical simulations to compute optimal properties of the drug.

A general introduction to the use of PDEs to study how drug properties can be optimized by PDF analysis was first presented for a mathematical audience in [20]. In the present paper, we summarize the main results of [20] and add further examples. In particular, we now demonstrate how PDFs can be used to improve existing pharmacological therapies (i.e. lidocaine and mexiteline). The method introduced here provides very clear results regarding optimal theoretical properties of a drug which normalizes mutated ion channels with respect to wild-type function, and thereby offers a theoretical framework by which analyses can be used to advance understanding of a hypothetical therapeutic target. We also include a theoretical argument showing that the entire probability density function can be repaired by using the optimal drug.

2 Mathematical models and methods for analyzing single ion channel dynamics

In this section, we introduce mathematical methods for analyzing stochastic release of calcium from internal storage systems of the cardiac muscle cell to the dyad and the cytosol. This process can be described using a Markov model and an associated equation which keeps track of the dyadic calcium concentration. Mutations of interest are modeled by changing the rates of the Markov models, [16–19]. In particular, we will use the concept of the *mutation severity index* (see [20]) to express the magnitude of the mutations. In addition to being ideal for modeling channel mutation, Markov models are also very well-suited to represent the effects of drugs on the channels [21, 23, 31–33]; models can be used to assess the quality of existing drugs and to give indications of how drug properties might be changed to obtain improved efficiency. Analysis of channel properties can be done using Monte Carlo simulations, essentially amounting to running a huge number of simulations and then computing the average dynamics of concentration. A much more elegant and powerful method is available: the PDF of the states of the Markov model can be computed by solving a system of PDE [20, 28, 29, 34–36]. This method can be applied when the Markov model is extended to account for drug effects and represents a powerful tool for both analyzing the effect of existing drugs and looking for improved drugs.

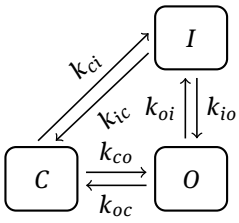

Figure 1: A three state Markov model Markov model including three possible states: open (O), closed (C), and inactivated (I).

Generally, it is desirable to use a drug to reduce the effect of a mutation. Therefore, we aim at tuning the parameters of a given drug such that the drugged channel behaves as close as possible to the wild-type channel. Moreover, we use the distance to the wild type solution as a way of measuring the quality of a given drug, as detailed below.

2.1 A simple Markov model

The simplest possible Markov model takes the form

$$C \underset{k_{co}}{\overset{k_{oc}}{\leftrightarrows}} O, \tag{1}$$

where k_{oc} and k_{co} are reaction rates. The rate k_{oc} express the likelihood that a channel changes state from open to closed during a brief time interval. Similarly, the rate k_{co} is the likelihood for a closed channel to become open during a given small interval of time. This can be expressed more formally by letting $S = S(t)$ denote a random variable representing the state of the channel (either closed C or open O) at time t. With this notation, the transition rates k_{oc} and k_{co} give the probability of changing state during the small time interval Δt :

$$k_{oc}\Delta t = \text{Prob}\left[S(t+\Delta t) = C \mid S(t) = O\right]$$

and

$$k_{co}\Delta t = \text{Prob}\left[S(t+\Delta t) = O \mid S(t) = C\right],$$

As shown below, these rates prove very useful as tools to manipulate properties of the Markov model (1).

2.1.1 A Markov model with three states

The concept of a Markov model is easily extended to situations where it is natural to include many more states in the model. On example is given in Figure 1, where a Markov model with three states is given. Here O denotes the open state, C is the closed state, and I is an inactivated state. In our analysis of applications below, we will address much more complex Markov models involving many states.

2.2 The master equation

From the Markov model (1), it is well-known [6, 7] that a master equation can be derived which governs the probability of being in the open or closed state (see e.g. [20, 28, 37]). If we assume that the rates k_{oc} and k_{co} are constant, the master equation for the simple model (1) then takes the form

$$o'(t) = k_{co}c(t) - k_{oc}o(t) \tag{2}$$

$$c'(t) = k_{oc}o(t) - k_{co}c(t). \tag{3}$$

By using the fact that the probabilities must add up to one, $o(t) + c(t) = 1$, this 2×2 system can be reduced to a scalar ordinary differential equation. Similarly, the master equation of the three-state model illustrated in Figure 1 can be written on the form

$$\begin{aligned} o' &= k_{io} i + k_{co} c - (k_{oi} + k_{oc})\, o, \\ c' &= k_{oc} o + k_{ic} i - (k_{co} + k_{ci})\, c, \\ i' &= k_{oi} o + k_{ci} c - (k_{io} + k_{ic})\, i. \end{aligned} \tag{4}$$

Again, the system size can be reduced from 3×3 to 2×2 by using the fact that the probabilities must sum to one.

2.3 The equilibrium solution

It is instructive to consider the equilibrium solution of these models. In the simple 2×2 model (1), the equilibrium probabilities are characterized by the following equation

$$k_{co} c = k_{oc} o.$$

As probabilities add up to one, we find that

$$o = \frac{k_{co}}{k_{co} + k_{oc}} \text{ and } c = \frac{k_{oc}}{k_{co} + k_{oc}}. \tag{5}$$

For the 3×3 model given in Figure 1, the equilibrium solution is characterized by the equations

$$k_{co} c = k_{oc} o,\ k_{oi} o = k_{io} i,\ k_{ic} i = k_{ci} c. \tag{6}$$

Again, since $o + c + i = 1$, we find that

$$o = \frac{1}{1 + \frac{k_{oc}}{k_{co}} + \frac{k_{oi}}{k_{io}}},\ c = \frac{\frac{k_{oc}}{k_{co}}}{1 + \frac{k_{oc}}{k_{co}} + \frac{k_{oi}}{k_{io}}},\ i = \frac{\frac{k_{oi}}{k_{io}}}{1 + \frac{k_{oc}}{k_{co}} + \frac{k_{oi}}{k_{io}}}. \tag{7}$$

2.3.1 Detailed balance

It follows from the equilibrium conditions (6) that the rates of the Markov model must satisfy the condition

$$k_{co} k_{oi} k_{ic} = k_{ci} k_{io} k_{oc}. \tag{8}$$

This relation is referred to as the condition of *detailed balance*, see e.g. [37].

2.3.2 Mean open time

The mean open time of the channel is determined by the rates leaving the open state; see e.g. [20, 28]. Specifically, for the 2×2 model (1), the mean open time is given by

$$\tau_o = \frac{1}{k_{oc}}, \tag{9}$$

and for the 3×3 model illustrated in Figure 1, the mean open time is given by

$$\tau_o = \frac{1}{k_{oc} + k_{oi}}. \tag{10}$$

2.4 The mutation severity index

As previously noted, mutations may significantly change ion channel properties and this effect can often be modeled by changing the state transition rates of the Markov model (see e.g. [16]). In the simplest case, the effect of a mutation might be to increase the closed to open rate, resulting in the Markov model,

$$C \underset{\mu k_{co}}{\overset{k_{oc}}{\leftrightarrows}} O, \tag{11}$$

where μ is referred to as the mutation severity index. Here, $\mu = 1$ is the wild type case; for $\mu > 1$, the rate from close to open is increased. Note that for the mutation, the equilibrium open probability is given by

$$o_\mu = \frac{\mu k_{co}}{\mu k_{co} + k_{oc}} = \frac{1}{1 + \frac{k_{oc}}{\mu k_{co}}}, \tag{12}$$

so clearly, o_μ approaches 1 as $\mu \to \infty$.

The mutation modeled by (11) does not affect the mean open time, but a mutation affecting the rate from the open to the closed state will. For instance, if the mutation increase the rate from O to C, we get a Markov model of the form

$$C \underset{k_{co}}{\overset{\mu k_{oc}}{\leftrightarrows}} O, \tag{13}$$

with equilibrium open probability given by

$$o_\mu = \frac{1}{1 + \frac{\mu k_{oc}}{k_{co}}}, \tag{14}$$

and the mean open time is given by

$$\tau_o = \frac{1}{\mu k_{oc}}. \tag{15}$$

For this mutation, we note that as $\mu \to \infty$, the equilibrium open probability goes to zero and thus so does the mean open time.

2.5 Markov models of drug effects

Markov models have been applied successfully to model the effects of various drugs; see e.g. [20, 21, 23, 31–33, 38]. A schematic of the modeling approach is illustrated in Figure 2; a new drugged state, D, is included in the model. This state may be either conducting (open, D_O) or non-conducting (closed, D_C). Suppose, for instance, that we consider the model (11) and we want to improve the properties of the channel by a drug associated to the closed state as follows

$$D_C \underset{k_{dc}}{\overset{k_{cd}}{\leftrightarrows}} C \underset{\mu k_{co}}{\overset{k_{oc}}{\leftrightarrows}} O. \tag{16}$$

Clearly, the properties of the drug are given by the rates k_{dc} and k_{cd}. By following the steps outlined above, we find that the open probability in the presence of the drug is given by

$$o_{\mu,d} = \left(1 + \frac{k_{oc}}{k_{co}} \frac{1}{\mu} \left(1 + \frac{k_{cd}}{k_{dc}}\right)\right)^{-1}. \tag{17}$$

From (5) we have that the equilibrium open probability of the wild type channel is given by

$$o = \left(1 + \frac{k_{oc}}{k_{co}}\right)^{-1}. \tag{18}$$

By comparing the formulas (17) and (18) for the open probabilities, we find that the drug can repair the equilibrium open probability of the mutant case completely if we choose the rates of the drug such that

$$\frac{1}{\mu} \left(1 + \frac{k_{cd}}{k_{dc}}\right) = 1, \tag{19}$$

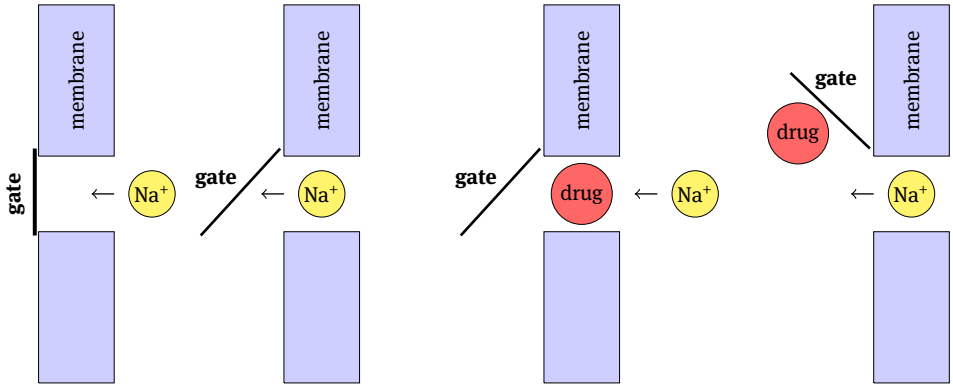

Figure 2: Gating of the sodium channel From left to right: 1) The gate of the channel is closed (the Markov model is in the closed state) and no sodium ions will pass through the channel. 2) The gate is open (the Markov model is in the open state) and sodium flows freely through the channel. 3) A drug is used to closed the channel (the Markov model is in a non-conducting state). 4) A drug is used to open the channel (the Markov model is in a conducting state). The figure is based on a figure in [32].

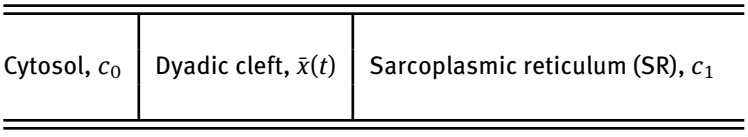

Figure 3: Model of calcium concentration The calcium concentration c_1 of the sarcoplasmic reticulum (SR) is assumed to be very large and constant. A channel is located between the SR and the dyadic cleft. The channel can be open or closed, depending on the state of the Markov model. When the channel is open, calcium flows into the dyadic cleft because of the concentration gradient. Furthermore, calcium diffuses from the dyadic cleft to the cytosol. The cytosolic space is assumed to be very large and therefore the concentration is assumed to be constant (c_0). □

or

$$\frac{k_{cd}}{k_{dc}} = \mu - 1. \tag{20}$$

Any drug that satisfies the relation as defined above will completely repair the equilibrium open probability of the channel with respect to wild type function. Furthermore, in the case of $\mu = 1$ (wild type), the optimal drug is actually no drug: $k_{cd} = 0$, providing reassuring evidence of the method's reasonableness.

2.6 Stochastic model of calcium concentration

We will now use the Markov models introduced above to analyze a prototype model of stochastic release of calcium from an intracellular storage system of the cardiac muscle cell. A sketch outlining the model is given in Figure 3, and the associated stochastic model of the calcium concentration $\bar{x} = \bar{x}(t)$ of the dyadic cleft is given by

$$\bar{x}'(t) = \bar{\gamma}(t)v_r(c_1 - \bar{x}) + v_d(c_0 - \bar{x}). \tag{21}$$

Here, the first term on the right hand side models influx of calcium from the SR to the intracellular space; $\bar{\gamma}$ is a stochastic variable governed by a Markov model. It is assumed to take on two possible values; $\bar{\gamma} = 1$ when the channel is open, and $\bar{\gamma} = 0$ when the channel is closed. When the channel is open, v_r denotes the speed of the release. Finally, v_d denotes the speed of diffusion from the dyadic cleft to the cytosol. The properties of (21) can be analyzed by Monte Carlo simulation; the results of repeated runs can be added in order to estimate the probability density functions of the states of the Markov model. These probability density functions can, however, also be computed by direct solution of a deterministic system of partial differential equations.

2.7 Probability density functions

A powerful way of analyzing the calcium dynamics governed by the stochastic model (21) is to compute the probability density function of the states of the Markov model directly. We consider the Markov model (1) and the stochastic model (21), and we let $\rho_o = \rho_o(x, t)$ denote the probability density functions (PDFs) of the channel in an open state; similarly, $\rho_c = \rho_c(x, t)$ denotes the PDFs of the channel being in a closed state. Now, the probability of the channel being open and the concentration $\bar{x} = \bar{x}(t)$ being in the interval $(x, x+\Delta x)$ at time t is given by

$$P_o\left\{x < \bar{x}(t) < x + \Delta x\right\} = \int_x^{x+\Delta x} \rho_o(\xi, t)\, d\xi. \tag{22}$$

Similarly, we have

$$P_c\left\{x < \bar{x}(t) < x + \Delta x\right\} = \int_x^{x+\Delta x} \rho_c(\xi, t)\, d\xi. \tag{23}$$

Following [20, 27, 28], we find that the PDFs are governed by the following linear system of partial differential equations,

$$\frac{\partial \rho_o}{\partial t} + \frac{\partial}{\partial x}(a_o \rho_o) = k_{co}\rho_c - k_{oc}\rho_o, \tag{24}$$

$$\frac{\partial \rho_c}{\partial t} + \frac{\partial}{\partial x}(a_c \rho_c) = k_{oc}\rho_o - k_{co}\rho_c, \tag{25}$$

with boundary conditions

$$\frac{\partial \rho_o}{\partial n} = \frac{\partial \rho_c}{\partial n} = 0$$

on either end, and where

$$\begin{aligned} a_o(x) &= v_r(c_1 - x) + v_d(c_0 - x), \\ a_c(x) &= v_d(c_0 - x). \end{aligned} \tag{26}$$

2.7.1 Numerical solution

The problem (24,25) can be solved using well know numerical methods. Our approach (see [20]) to the problem is to write the system on the form

$$\rho_t + (A\rho)_x = K\rho \tag{27}$$

with,

$$\rho = \begin{pmatrix} \rho_o \\ \rho_c \end{pmatrix},\ A = \begin{pmatrix} a_o & 0 \\ 0 & a_c \end{pmatrix},\ \text{and } K = \begin{pmatrix} -k_{oc} & k_{co} \\ k_{oc} & -k_{co} \end{pmatrix}. \tag{28}$$

When the system is written on this form, it can be solved using operator splitting (see e..g. [39–41]). The system will then be solved in two steps; one step solves the hyperbolic and space dependent part, and the second step solves a system of ordinary differential equations.

Let ρ^n be the solution at time $t_n = n\Delta t$. Then, the first step is to solve the hyperbolic system

$$\rho_t + (A\rho)_x = 0 \tag{29}$$

from $t = t_n$ to $t = t_n + \Delta t$. For the second step, we use this solution to define the initial condition; $u(t_n) = \rho(t_{n+1})$, and solve the ordinary differential equations given by

$$u_t = Ku \tag{30}$$

from $t = t_n$ to $t = t_n + \Delta t$. Finally, we update the solution by defining

$$\rho_{n+1} = u(t_{n+1}). \tag{31}$$

The problem of solving the system (24,25) is now reduced to solve a standard, linear hyperbolic problem and to solve a system of ordinary differential equations. In addition, the system of hyperbolic equations decouples completely and consists of two, scalar equations that can be solved separately. Numerical methods for hyperbolic problems is covered in [39], and numerical methods for solving systems of ordinary differential equations can be found most textbooks on numerical methods; see e.g. [42, 43].

2.8 Probability density functions for a three state model

The system above governing the PDFs of the open and closed states can, in principle, be extended to cover any Markov model. In order to indicate how to generalize the system , we consider the Markov model given in Figure 1 and note that the PDFs are governed by the system (see [20], ch. 11)

$$\frac{\partial \rho_o}{\partial t} + \frac{\partial}{\partial x}(a_o \rho_o) = k_{co}\rho_c - (k_{oc} + k_{oi})\rho_o + k_{io}\rho_i, \tag{32}$$

$$\frac{\partial \rho_c}{\partial t} + \frac{\partial}{\partial x}(a_c \rho_c) = k_{oc}\rho_o - (k_{co} + k_{ci})\rho_c + k_{ic}\rho_i, \tag{33}$$

$$\frac{\partial \rho_i}{\partial t} + \frac{\partial}{\partial x}(a_c \rho_i) = k_{oi}\rho_o - (k_{io} + k_{ic})\rho_i + k_{ci}\rho_c, \tag{34}$$

where a_o and a_c are given by (26).

2.8.1 Probability density functions in the presence of a drug

The PDF can also be computed for the Markov model (16). In this case the probability density functions are governed by the system

$$\frac{\partial \rho_o}{\partial t} + \frac{\partial}{\partial x}(a_o \rho_o) = \mu k_{co}\rho_c - k_{oc}\rho_o, \tag{35}$$

$$\frac{\partial \rho_c}{\partial t} + \frac{\partial}{\partial x}(a_c \rho_c) = k_{oc}\rho_o - (\mu k_{co} + k_{cd})\rho_c + k_{dc}\rho_d, \tag{36}$$

$$\frac{\partial \rho_d}{\partial t} + \frac{\partial}{\partial x}(a_c \rho_d) = k_{cd}\rho_c - k_{dc}\rho_d, \tag{37}$$

where, again, a_o and a_c are given by (26).

3 Applications of models and methods

In this section, we will use the described to demonstrate how optimal properties of theoretical compounds can be computed via drug model parameter tuning. We will first consider a generic two-state Markov model and show theoretically that the effect of a mutation can be repaired completely. Next, we consider a two-state Markov model of the cardiac ryanodine receptor (RyR2) channel. This model is easily extended to describe the theoretical application of a drug. Finally, to show that the outlined methods will generalize well to more complex Markov channel models, we will consider an eight-state Markov model of the fast sodium channel and use the developed framework for computing optimal drugs.

3.1 Example: a two-state Markov model as the simplest possible case

We illustrate the methods described above for a very simple, generic case. Consider the two-state Markov model (1) and the associated system of partial differential equations (PDEs) (24,25) governing the probability density functions (PDFs) of the open and closed states. As mentioned above, the PDFs can be computed by

Table 1: Parameters of the models (1) and (21). □

ν_d	$0.1\ \text{ms}^{-1}$
ν_r	$1\ \text{ms}^{-1}$
c_0	$0.1\ \mu\text{M}$
c_1	$1000\ \mu\text{M}$
k_{co}	$0.2\ \text{ms}^{-1}$
k_{oc}	$1\ \text{ms}^{-1}$

performing a large number of Monte Carlo (MC) simulations based on the model (21), or by solving the system (24,25). In Figure 4, we show the stationary solutions using these two methods; the histograms represent the MC solutions, and the solid green lines represent the PDFs computed by solving (24,25). The parameters used in computation are given in Table 1. Numerical methods for solving the system (24,25) is discussed above, and details of how to compute the histograms are given in [20]. In the figure, we observe that the MC simulations (histograms) and the solution of the system of PDEs (solid lines) provide the same solution, and that the introduced mutation leads to increased open probability.

3.1.1 The effect of the mutation and its reversal with application of a theoretical drug

In the Markov model (11), we introduced the effect of a mutation; the effect of a closed state drug was added in (16). Furthermore, the system modeling the PDFs of the states are given in (35)-(37). In Figure 5, we show the stationary solutions of the wild type channel (green), the mutated channel (red) and the mutation after the application of the drug (blue; three versions). In the computations of the drugged case, drug parameters satisfy (20), i.e. we have used $k_{cd} = (\mu - 1)k_{dc}$ for three versions of the parameter k_{dc}. We note that the drug works with improved efficacy as the value of k_{dc} increases; in fact, it can be shown mathematically (see [20], page 63) that as $k_{dc} \to \infty$, the PDF of the open state for the mutant channel converges to the PDF of the wild type channel and thus, asymptotically, the channel is perfectly repaired.

3.2 Mutation in the cardiac ryanodine receptor affecting calcium release

Next, we consider the simple two-state Markov model of Cannell et al. [44] to model a catecholaminergic polymorphic ventricular tachycardia (CPVT) mutation in the cardiac ryanodine receptor (RyR2) channel. In particular, we use data from Zhao et al. [45] to define a model of the CPVT mutation RyR2-A4860G that reduces channel open probability. The Markov model takes the form

$$C \underset{\mu k_{oc}}{\overset{k_{co}}{\rightleftarrows}} O \underset{k_{do}}{\overset{k_{od}}{\rightleftarrows}} D_O \tag{38}$$

where the rates depend on the dyadic calcium concentration c;

$$k_{co}(c) = k_{co}^{-} + \frac{k_{co}^{+} - k_{co}^{-}}{1 + (c/\bar{c}_{co})^{s_{co}}},$$

and

$$k_{oc}(c) = k_{oc}^{-} + \frac{k_{oc}^{+} - k_{oc}^{-}}{1 + (c/\bar{c}_{oc})^{s_{oc}}}.$$

In the Cannell et al. model [44] these rates are only piecewise smooth, while here we have reparameterized them to obtain globally smooth rates. The parameters are given in Table 2. The stochastic equation governing the calcium concentration is given by

$$\frac{dc}{dt} = \gamma(t) g_{RyR}(c_1 - c) + g_L(c_0 - c) \tag{39}$$

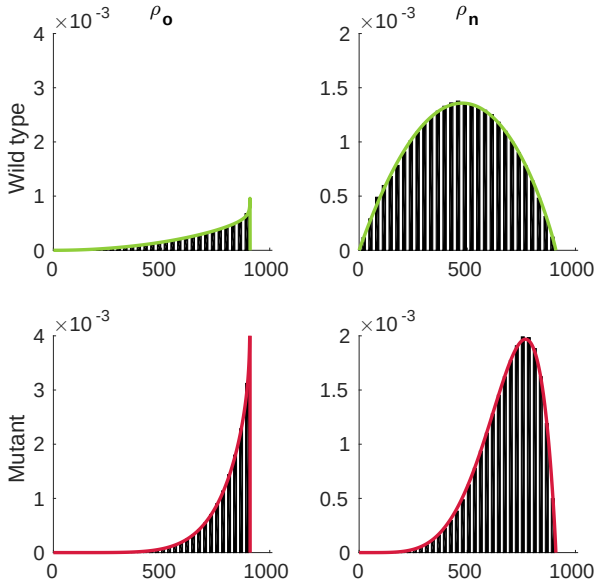

Figure 4: Probability density functions vs. Monte Carlo distributions Upper left panel: The probability density function of the open state for a wild type channel, computed by solving the system of partial differential equations (35)-(37) (solid green line), and the solution computed by repeated Monte Carlo simulations (histogram). Upper right panel: The probability density function of the non-conducting (closed) state. Lower panels: The mutant case. In the computations we have used mutation severity index $\mu = 3$. □

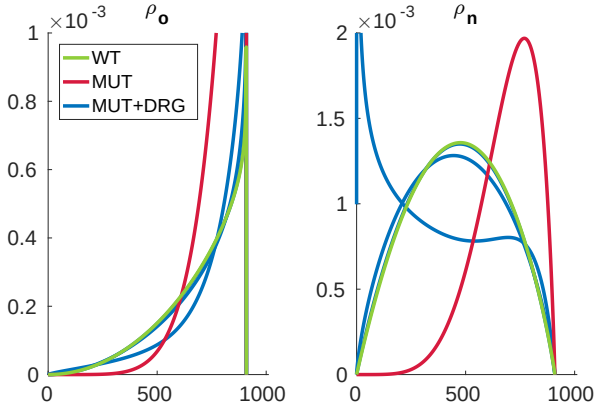

Figure 5: Wild type, mutant and drug effect The probability density functions for the wild type (green) channel, mutant channel (red) and the mutant channel + drug (blue), of the open (left) and the non-conducting (closed) states (right), computed by solving the system of partial differential equations. Three versions of the drug are used (blue lines), defined by $k_{dc} = 0.1, 1, 10$ and $k_{cd} = (\mu - 1)k_{dc}$. □

Table 2: Parameters of the Markov model (38). □

k_{co}^{-}	$1 \cdot 10^{-3}\text{ms}^{-1}$	k_{oc}^{-}	1ms^{-1}
k_{co}^{+}	0.5ms^{-1}	k_{oc}^{+}	10ms^{-1}
$\bar{c}_{co}$	$50\mu\text{M}$	$\bar{c}_{co}$	$50\mu\text{M}$
s_{co}	-3	s_{co}	1

where $g_L = 0.1\text{ms}^{-1}$, $g_{RyR} = 0.1\text{ms}^{-1}$, $c_0 = 1\mu\text{M}$, $c_1 = 1000\mu\text{M}$, and finally $\gamma = \gamma(t)$ is zero or one, depending on the state of the Markov model as explained in Methods.

3.2.1 Characterizing optimal drugs using probability density functions

The system governing the PDFs of the O, C and D_O states takes the form

$$\frac{\partial \rho_o}{\partial t} + \frac{\partial}{\partial x}(a_o \rho_o) = k_{co}\rho_c - (\mu k_{oc} + k_{od})\rho_o + k_{do}\rho_d, \tag{40}$$

$$\frac{\partial \rho_c}{\partial t} + \frac{\partial}{\partial x}(a_c \rho_c) = \mu k_{oc}\rho_o - k_{co}\rho_c, \tag{41}$$

$$\frac{\partial \rho_d}{\partial t} + \frac{\partial}{\partial x}(a_o \rho_d) = k_{od}\rho_o - k_{do}\rho_d. \tag{42}$$

Since both the O and the D_O states are open (conducting), we can define the combined open probability density function

$$\rho_\star = \rho_o + \rho_d.$$

By adding (40) and (42) we find that the the PDFs $\rho_\star$ and ρ_c are governed by the system

$$\frac{\partial \rho_\star}{\partial t} + \frac{\partial}{\partial x}(a_o \rho_\star) = k_{co}\rho_c - \mu k_{oc}\rho_o \tag{43}$$

$$\frac{\partial \rho_c}{\partial t} + \frac{\partial}{\partial x}(a_c \rho_c) = \mu k_{oc}\rho_o - k_{co}\rho_c, \tag{44}$$

It is useful to define

$$\alpha = \frac{k_{od}}{k_{do}}$$

and observe that (42) can be written on the form

$$\frac{1}{k_{do}}\left(\frac{\partial \rho_d}{\partial t} + \frac{\partial}{\partial x}(a_o \rho_d)\right) = \alpha\rho_o - \rho_d.$$

If we assume that the drug k_{do} rate is very fast, we have $\rho_d \approx \alpha\rho_o$, and therefore

$$\rho_\star = \rho_o + \rho_d \approx (\alpha + 1)\rho_o,$$

so we can rewrite the system (43) – (44) on the form

$$\frac{\partial \rho_\star}{\partial t} + \frac{\partial}{\partial x}(a_o \rho_\star) = k_{co}\rho_c - \frac{\mu}{\alpha + 1}k_{oc}\rho_\star \tag{45}$$

$$\frac{\partial \rho_c}{\partial t} + \frac{\partial}{\partial x}(a_c \rho_c) = \frac{\mu}{\alpha + 1}k_{oc}\rho_\star - k_{co}\rho_c, \tag{46}$$

If we choose α such

$$\frac{\mu}{\alpha + 1} = 1$$

we observe that the system (45) – (46) is identical to the system governing the wild type PDFs,

$$\frac{\partial \rho_o}{\partial t} + \frac{\partial}{\partial x}(a_o \rho_o) = k_{co}\rho_c - k_{oc}\rho_o \tag{47}$$

$$\frac{\partial \rho_c}{\partial t} + \frac{\partial}{\partial x}(a_c \rho_c) = k_{oc}\rho_o - k_{co}\rho_c, \tag{48}$$

and therefore the drug repairs the mutant channel completely, theoretically, provided that the rates are very fast and

$$k_{od} = (\mu - 1)\, k_{do}. \tag{49}$$

3.2.2 Numerical simulations

In Figure 6, we show the PDFs of the open and non-conducting states for the wild type channel (green), the mutant channel (no drug, red), and mutant channel after the drug is applied (blue). Again, we note that the solutions computed by doing repeated Monte Carlo simulations (histograms) and solving the deterministic system of PDFs (solid lines) provide very similar solutions. Furthermore, we see that the mutation significantly decreases open probability and increases the probability of being in the closed state. The introduction of the drug seems to repair the effect of the mutation i.e. restores open probability of the channel, approximating wild type channel behavior. In the numerical computation, we have used the mesh size $\Delta c = 0.057\mu$M, and the time step used in solving (39) was $\Delta t = 1\mu s$.

In Figure 7, we show the solution of the system (40)-(42) for three values of the drug parameters; $k_{do} = 0.1, 1, 10$, and $k_{od} = (\mu - 1)\, k_{do}$. As expected, as the rates increase, the solution of the mutant channel + drug behaves similarly to the wild type solution.

The Markov model (38) was implemented to handle the RyR-release in the whole cell model presented in Chapter 15 of [20]. The results are given in Figure 8. We note that the mutation significantly affects the dyadic calcium concentration, and that the effect of the mutation is predominantly removed when the drug is applied.

3.3 Model of calcium release depending on both c_i and c_s

Next, we consider the two-state Markov model for the ryanodine receptor, RyR from [46]:

$$C \underset{k_{oc}}{\overset{\mu k_{co}}{\rightleftarrows}} O \tag{50}$$

where the transition rates depend on both the dyadic calcium concentration, c_i, and the sarcoplasmic reticulum (SR) calcium concentration, c_s:

$$k_{co}(c_i, c_s) = k^+(\phi_b + (c_s/\phi_k)^4)c_i^\eta$$

and

$$k_{oc} = k^-.$$

The constants are given in Table 3.

The stochastic equations governing the calcium concentrations are given by

$$\frac{dc_i}{dt} = \gamma(t) g_{RyR}(c_s - c_i) + g_L(c_0 - c_i) \tag{51}$$

$$\frac{dc_s}{dt} = \gamma(t) g_{RyR}(c_i - c_s) + g_F(c_1 - c_s) \tag{52}$$

where $g_F = 0.1$, $g_L = 0.1\text{ms}^{-1}$, $g_{RyR} = 0.1\text{ms}^{-1}$, $c_0 = 0.1\mu$M, $c_1 = 1000\mu$M, and finally $\gamma = \gamma(t)$ is zero or one depending on the state of the Markov model.

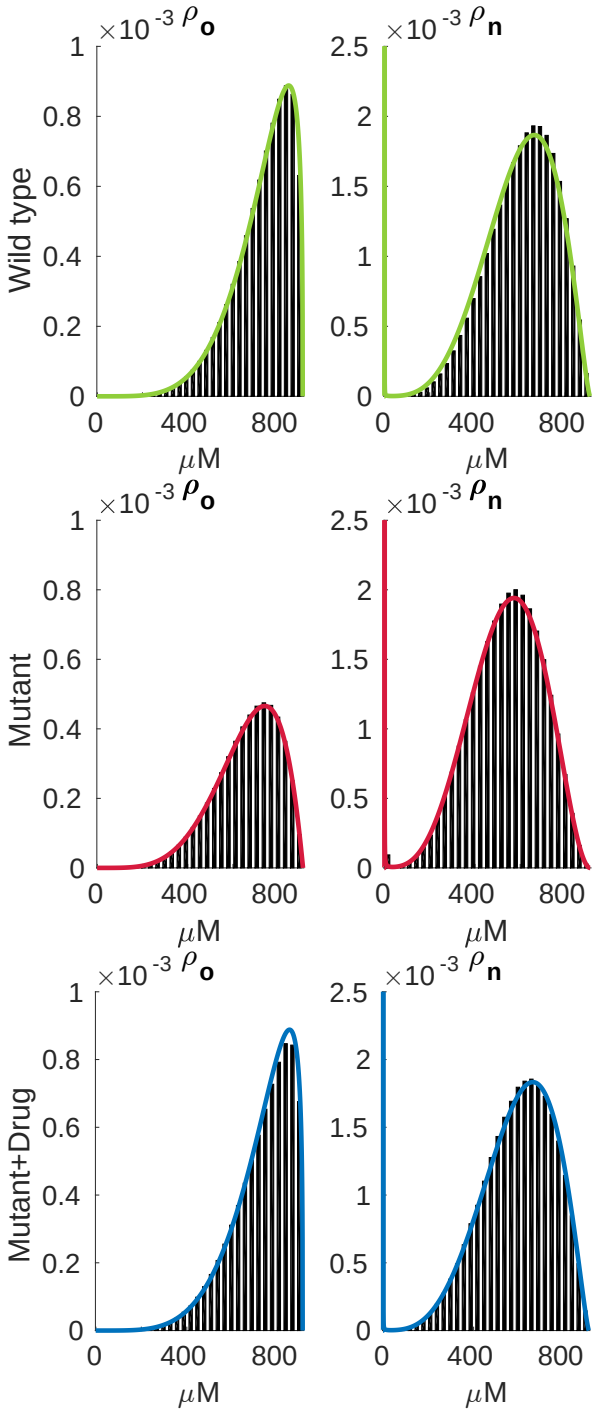

Figure 6: Probability density functions and Monte Carlo distributions Probability density functions of the open and non-conducting states for the wild type channel (upper), mutant channel (middle) and mutant channel + drug (lower). In the simulations we have used $\mu = 1.5$, $k_{od} = 10\text{ms}^{-1}$and $k_{do} = 20\text{ms}^{-1}$. □

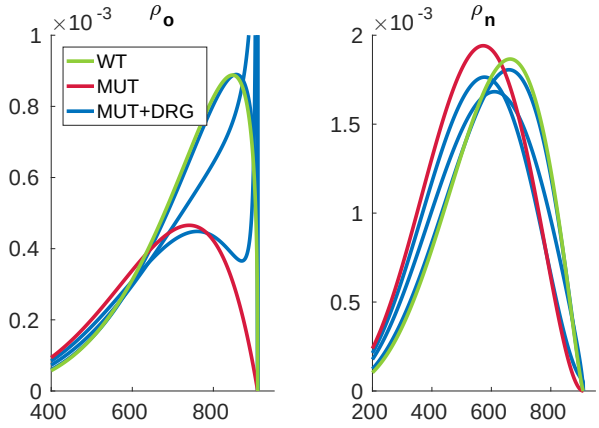

Figure 7: Wild type, mutant and drug The probability density function of the open states ($\rho_o + \rho_d$, left) and the non-conducting (closed) state (right). Three rates are used $k_{do} = 0.1, 1, 10$, and $k_{od} = (\mu - 1)\, k_{do}$. □

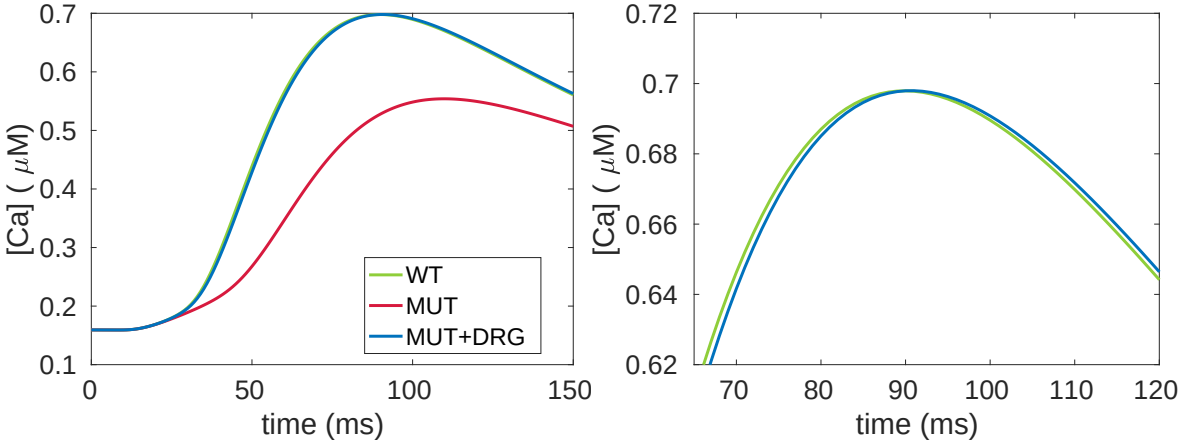

Figure 8: Calcium transient Whole cell simulation using the RyR release model given by (38). At left: The calcium concentration of the dyad for the wild type channel, mutant channel and mutant channel + drug. In the simulations, we have used $k_{od} = 1$, $k_{do} = 2$. Right: Zooming in on the time interval ranging from 60 to 120ms; we note the even for these slow rates, the drug almost completely repairs the calcium concentration in the dyad. □

Table 3: Parameters of the Markov model from Walker et al [46].

k^-	0.5ms^{-1}
k^+	$1.107 \cdot 10^{-4}\text{ms}^{-1^{-1}}\mu\text{M}^{-\eta}$
ϕ_k	1.5mM
ϕ_b	0.8025
η	2.1

The corresponding PDF system is:

$$\frac{\partial \rho_o}{\partial t} + \frac{\partial}{\partial c_i}\left(a_o^{c_i}\rho_o\right) + \frac{\partial}{\partial c_s}\left(a_o^{c_s}\rho_o\right) = k_{co}\rho_c - k_{oc}\rho_o, \tag{53}$$

$$\frac{\partial \rho_c}{\partial t} + \frac{\partial}{\partial c_i}\left(a_c^{c_i}\rho_c\right) + \frac{\partial}{\partial c_s}\left(a_c^{c_s}\rho_c\right) = k_{oc}\rho_o - k_{co}\rho_c, \tag{54}$$

where

$$\begin{aligned} a_o^{c_i} &= g_{RyR}\left(c_s - c_i\right) + g_L\left(c_0 - c_i\right), \\ a_o^{c_s} &= g_{RyR}\left(c_i - c_s\right) + g_F\left(c_1 - c_s\right), \\ a_c^{c_i} &= g_L\left(c_0 - c_i\right), \\ a_c^{c_s} &= g_F\left(c_1 - c_s\right). \end{aligned} \tag{55}$$

3.3.1 1D Numerical simulations

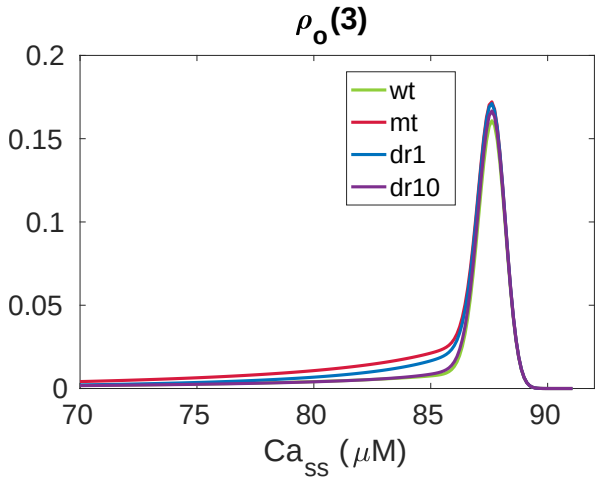

Figure 9: Wild type, mutant and two drugs The numbers in dr1 and dr10 refer to the values of k_{bc}. □

First, we keep c_s fixed, reducing the PDF computation to a 1D problem. Figure 9 shows the solution for $t = 3$ms. In this example, the mutation is causing an increased opening rate, represented with the mutation index $\mu > 1$:

$$k_{co,\mu} = \mu k_{co}$$

For the drug to repair the steady state, we know the rates should satisfy:

$$k_{cb} = (\mu - 1)k_{bc}$$

Furthermore, the larger the rates, the more closely we can approximate the wild type channel behavior with application of a theoretical drug. As expected $k_{bc} = 10$ is superior to $k_{bc} = 1$.

3.3.2 2D Numerical simulations

In Figure 10 we show the solution of the 2D problem defined in (53)-(55), at $t = 3$ms. Note that the mutant case (right panel) has a higher peak in open probability, and is wider compared to the wild type channel case (left panel). Figure 11 shows the effect of the applied drug. With $k_b c = 10$ the error becomes less than 4% (lower panel).

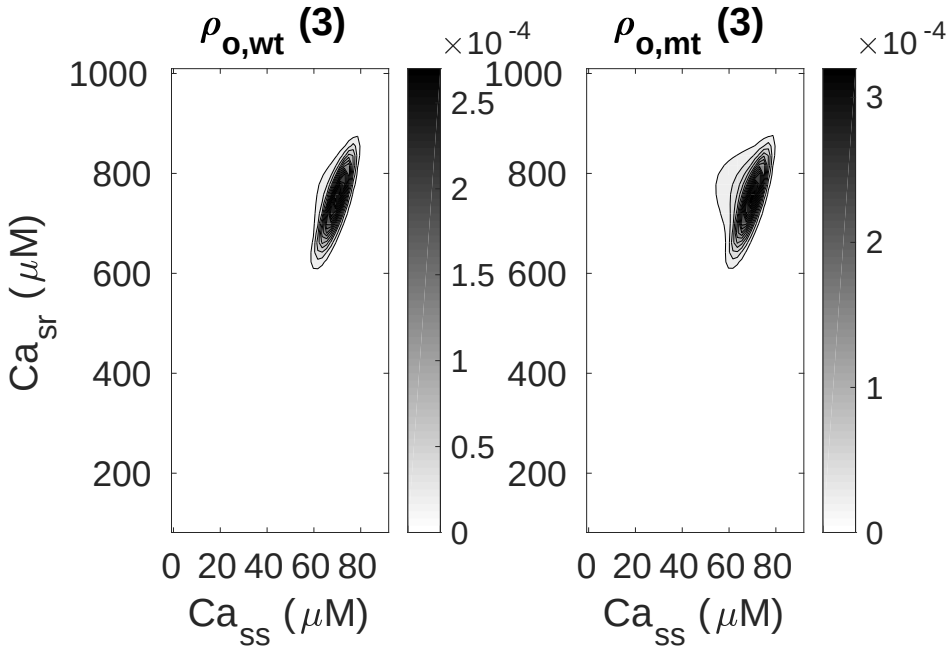

Figure 10: 2D probability density functions Solution of the problem defined in (53)-(55). Left: Wild type channel. Right: Mutant channel. □

3.4 The sodium channel

Table 4: The rate functions of the sodium channel model are taken from [16].□

Wild type						Mutant		
α_{1i}	=	$\frac{3.802}{0.1027\cdot e^{-V/p_{1i}}+p_{2i}\cdot e^{-V/150}}$	p_{11}	=	17	$\hat{\alpha}_{1i}$	=	$1.25\cdot\alpha_{1i}$
β_{1i}	=	$p_{3i}\cdot e^{-V/20.3}$	p_{12}	=	15	$\hat{\beta}_{1i}$	=	β_{1i}
α_2	=	$9.178\cdot e^{V/29.68}$	p_{13}	=	12	$\hat{\alpha}_2$	=	$9.178\cdot e^{V/100}$
β_2	=	$\frac{\alpha_{13}\cdot\alpha_2\cdot\alpha_3}{\beta_{13}\cdot\beta_3}$	p_{21}	=	0.20	$\hat{\beta}_2$	=	$\frac{\hat{\alpha}_{13}\cdot\hat{\alpha}_2\cdot\hat{\alpha}_3}{\hat{\beta}_{13}\cdot\hat{\beta}_3}$
α_3	=	$3.7933\cdot 10^{-9}e^{-V/5.2}$	p_{22}	=	0.23	$\hat{\alpha}_3$	=	$20\cdot\alpha_3$
β_3	=	$0.0084+0.00002V$	p_{23}	=	0.25	$\hat{\beta}_3$	=	$2\cdot\beta_3$
α_4	=	$\alpha_2/100$	p_{31}	=	0.1917	$\hat{\alpha}_4$	=	$\hat{\alpha}_2/100$
β_4	=	α_3	p_{32}	=	0.2552	$\hat{\beta}_4$	=	$\hat{\alpha}_3$
			p_{33}	=	0.3583	$\hat{\alpha}_0$	=	$2\cdot 10^{-6}$
						$\hat{\beta}_0$	=	$1\cdot 10^{-4}$

The first mathematical analysis of a mutation using a Markov model to represent the state of an ion channel was conducted by Clancy and Rudy, published in their seminal paper [16]. This Markov model was parameterized using data from Bennett et al. [48] and Chandra et al. [49]. The model represents the effect of the ΔKPQ mutation of the SCN5A gene of fast sodium channels. This mutation can lead to a characteristic late current, causing prolongation of the QT-interval; see e.g. [16]. In [23], Clancy, Zhu and Rudy introduced Markov models incorporating the effect of a variety of drugs. Theoretical analysis of potential pharmacotherapies was also analyzed in [50]. A key component of the Markov model presented by Clancy and Rudy is the burst mode. The Markov model is presented in Figure 12; we note that in the wild type case (upper panel), there are six states; one open state, two inactivated states and three closed states. In the mutant case, how-

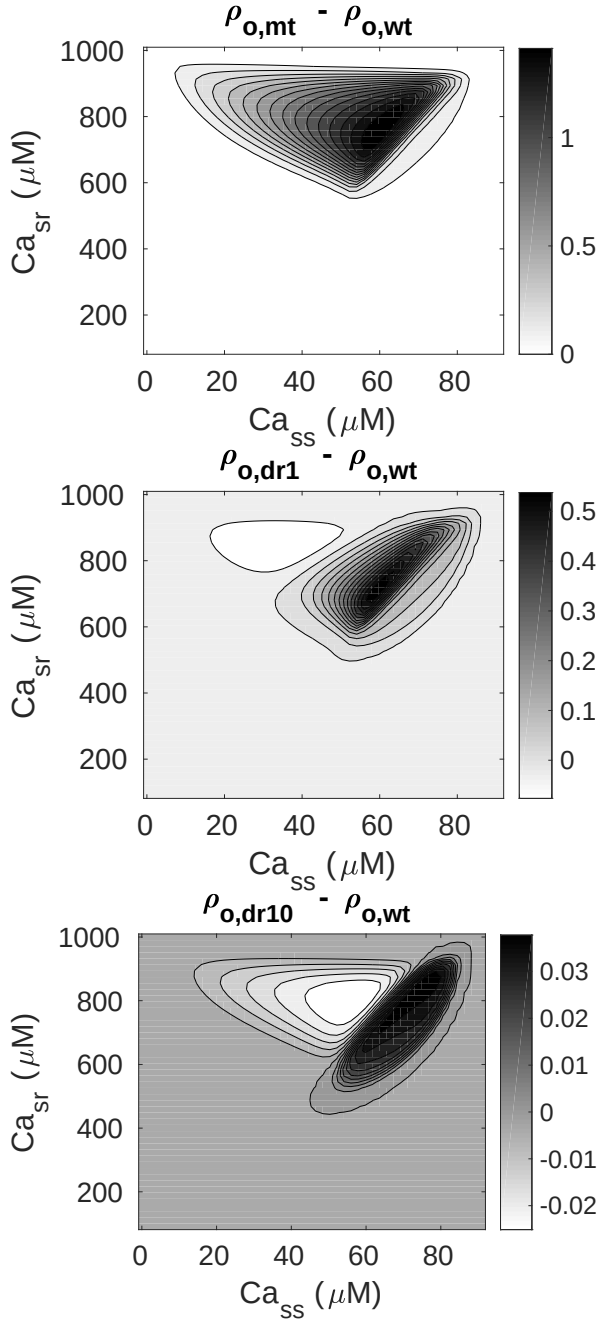

Figure 11: Distance to wild type The difference between wild type and mutant channel open probabilities, relative to the wild type channel. Top panel shows the non-drugged case with large discrepancies. The performance of the drug with $k_{bc} = 1$ and $k_{bc} = 10$ is shown in the next two channels, respectively. □

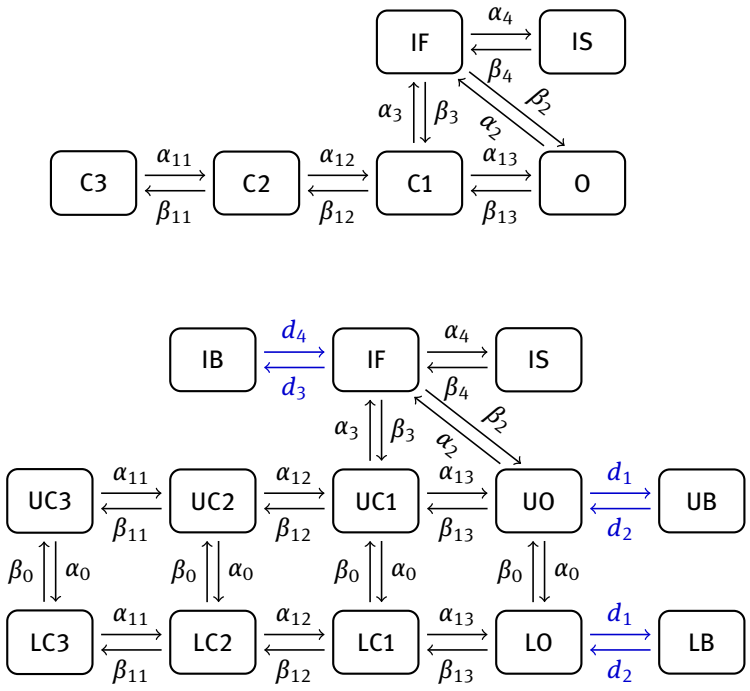

Figure 12: The Markov model of Clancy and Rudy [16]. Upper panel: The wild type channel model with six states; one open state (O), two inactivated states (IF, IS) and three closed states ($C1$, $C2$, $C3$). Lower panel: The mutant channel model is similar top the wild type channel model, but a burst mode is added involving one new open state and three new closed states. In the mutant model, drugs are included using the formalism proposed by Clancy, Zhu and Rudy [47]. The drug states are denoted IB, UB and LB, and the rates are given in blue.□

ever, (Figure 12, lower panel) a burst mode is added to the model; this burst mode has no inactivated states, meaning that the channel open probability increases slightly, which can lead to a characteristic late sodium current. Following Clancy et al. [23], we have introduced drugs associated with the open state and the inactivated states; see Figure 12, where reaction rates defining the drug appear in blue. The rates of the Markov model are given in Table 4.

3.4.1 Probability density functions

The transmembrane potential of a single sodium channel is governed by

$$\frac{dv}{dt} = \gamma g_{Na}(v_0 - v) + g_L(v_1 - v), \tag{56}$$

where $g_L = 0.1\text{ms}^{-1}$, $g_{Na} = 1\text{ms}^{-1}$, $v_0 = 40\text{mV}$, $v_1 = -85\text{mV}$, and, as above, the stochastic function γ is zero or one depending on the state of the Markov model. For the Markov models given in Figure 12, γ is one when the Markov model is in the state O for the model in the upper panel, and in the state UO or LO for the model given in the lower panel.

As explained in further detail in [20], we can formulate a system of partial differential equations (PDEs) modeling the probability density functions (PDFs) of the states of the Markov model;

$$\frac{\partial \rho_O}{\partial t} + \frac{\partial}{\partial v}(a_o \rho_O) = \beta_2 \rho_{IF} + \alpha_{13}\rho_{C1} - (\alpha_2 + \beta_{13})\rho_O, \tag{57}$$

$$\frac{\partial \rho_{IF}}{\partial t} + \frac{\partial}{\partial v}(a_c \rho_{IF}) = \alpha_2 \rho_O + \alpha_3 \rho_{C1} + \beta_4 \rho_{IS} - (\alpha_4 + \beta_2 + \beta_3)\rho_{IF}, \tag{58}$$

$$\frac{\partial \rho_{IS}}{\partial t} + \frac{\partial}{\partial v}(a_c \rho_{IS}) = \alpha_4 \rho_{IF} - \beta_4 \rho_{IS}, \tag{59}$$

$$\frac{\partial \rho_{C1}}{\partial t} + \frac{\partial}{\partial v}(a_c \rho_{C1}) = \beta_{13}\rho_O + \beta_3 \rho_{IF} + \alpha_{12}\rho_{C2} - (\alpha_3 + \alpha_{13} + \beta_{12})\rho_{C1}, \tag{60}$$

$$\frac{\partial \rho_{C2}}{\partial t} + \frac{\partial}{\partial v}(a_c \rho_{C2}) = \beta_{12}\rho_{C1} + \alpha_{11}\rho_{C3} - (\alpha_{12} + \beta_{11})\rho_{C2}, \tag{61}$$

$$\frac{\partial \rho_{C3}}{\partial t} + \frac{\partial}{\partial v}(a_c \rho_{C3}) = \beta_{11}\rho_{C2} - \alpha_{11}\rho_{C3}, \tag{62}$$

where

$$a_o = a_o(v) = g_{Na}(v_0 - v) + g_L(v_1 - v),$$

and

$$a_c = a_c(v) = g_L(v_1 - v).$$

Similarly, we can formulate at 13×13 system of PDEs modeling the PDFs of the Markov model given in the lower panel of Figure 12. Again, we refer to [20] for boundary conditions and numerical methods for solving the presented system. In Figure 13, we show the solution of this system of partial differential equations for the wild type channel, the mutant channel, and the mutant channel after a drug has been applied. The theoretical drug has been computed by minimizing the cost functional

$$J(d) = ||\rho^* - \rho(d)||_2 / ||\rho^*||_2 \tag{63}$$

where ρ^* is the wild type channel open probability distribution at $T = 10$ms, and $\rho(d)$ is the corresponding mutant channel distribution with the drug d applied. The best drug rates were identified by minimizing $J = J(d)$ at time $t = 10$ms (Fminsearch, Matlab). The optimal solution was found to be

$$(d_1, d_2, d_3, d_4) = (0.015869, 3.4938 \cdot 10^{-9}, 55.525, 0.14337)/\text{ms}.$$

The numerical solution was computed using a mesh with $\Delta V = 0.574$mV and time step 5μs.

The results given in Figure 13 show that the open probability is much larger in the mutant case than in for the wild type case, as expected. This effect can be almost completely repaired by the optimal theoretical drug, as shown.

3.4.2 Whole cell action potential

The PDF of the open state of the mutant sodium channel can be restored almost completely to its wild type phenotype by applying an optimal theoretical drug. Next, we will show how this theoretical therapy normalizes a whole cell action potential affected by the sodium channel mutation. We used the action potential model of Livshitz and Rudy [51] and applied the Markov model given in Figure 12 to represent the sodium channel. In Figure 14, we show the resulting action potential (left panel) and the associated sodium current (right panel). The characteristic late current of the ΔKPQ mutation is almost completely abolished by the theoretical drug, and, as a result, the undesired, excess depolarization of the whole cell action potential seen in the case of the mutant sodium channel is removed; the action potential of the mutant channel + drug is almost identical to the phenotype of the wild type channel case.

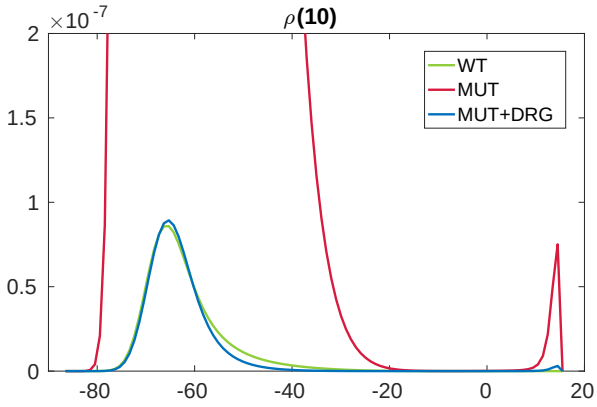

Figure 13: Wild type, mutant and drug Probability density functions at time $t = 10$ms of the open states for the wild type channel, mutant channel and mutant channel + optimal drug. The system (57)-(62) of partial differential equations gives the wild type solutions, whereas the the solutions mutant channel + drug case is defined by a 13×13 system of partial differential equations.□

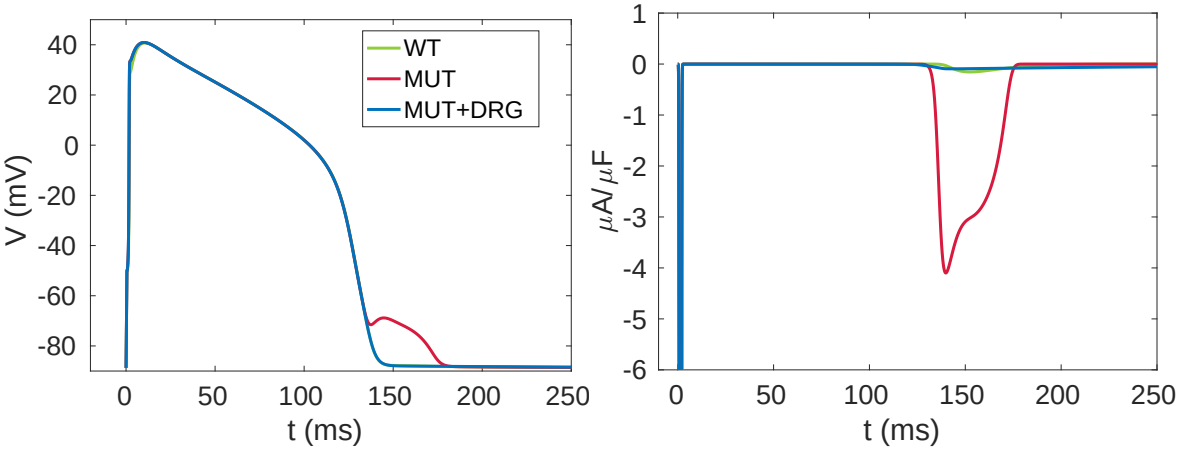

Figure 14: Action potential and sodium current Action potential (left panel) computed using the Livshitz and Rudy model [51] for the wild type channel, mutant channel and mutant channel + drug cases; the associated sodium currents are given in the right panel. The sodium channels are represented by the Markov model given in Figure 12. □

Table 5: The table gives rates applied in computations presented in Figure 15 and Figure 16. For the improved versions of lidocaine and mexiteline, we have used:
MEX: $\nabla J = (-1.0004, 128.49)$, $\epsilon = -1.945608 \cdot 10^{-3}$.
LID: $\nabla J = (-0.087658, 14.676)$, $\epsilon = -2.682 \cdot 10^{-2}$.

	d_1	d_2	d_3	d_4	$J(d)$
WT	-	-	-	-	0
MUT	-	-	-	-	663.62
MEX	100	0.25	-	-	125.49
MEX*	100	$3.9634 \cdot 10^{-6}$	-	-	0.5465
LID	-	-	100	0.4	14.713
LID*	-	-	100	0.1064825	0.11378
OPT	0.015869	$3.4938 \cdot 10^{-9}$	55.525	0.14337	0.0974012

3.5 Comparing existing and theoretical drugs

Several existing drugs for the sodium channel have been characterized using Markov models; see e.g. [23]. In Figure 15, we compare the open probability density function of these existing drugs with the theoretical drug derived in the previous section. In summary, we note that both lidocaine and mexiteline are able to improve the sodium channel open probability density functions, but not nearly as well as the optimal theoretical drug.

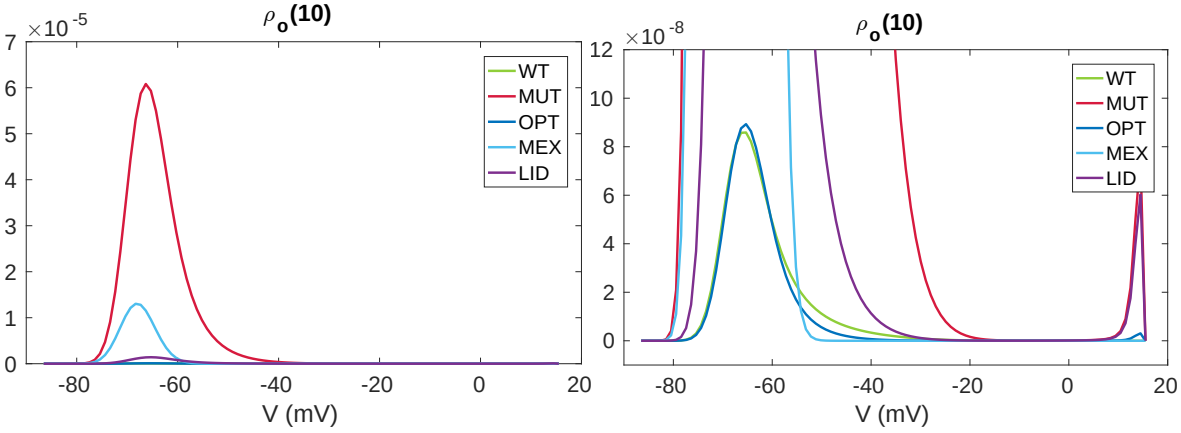

Figure 15: Wild type, mutant and three drugs Left panel: Wild type channel, mutant channel, and mutant channel + three different theoretical drugs (optimal, lidocaine and mexiteline). Right panel: Zoom of left panel. The rates of lidocaine and mexiteline are given in Table 5.

3.6 Improving existing drugs

A major challenge for translational applicability of theoretical drugs computed by the method introduced above is that we do not know whether it is physically possible to produce a drug with these properties given current drug development pipelines and technological limitations. However, it is potentially tractable to construct a drug with properties close to those of an existing drug, and we therefore show how the machinery developed above can be used to suggest improvements to a known drug. Suppose the rates of an existing drug are given by the vector d^*. Then the associated cost functional is given by $J(d^*)$ and we want to reduce this value by perturbing the rates d^*; we want to find a drug $D = d^* + d$. This can be done by applying a gradient

method to reduce the cost function. More specifically, the Taylor series expansion of the cost function reads

$$J(D) = J(d^\star + d) = J(d^\star) + \nabla J(d^\star) \cdot d + O(\|d\|^2),$$

and we therefore choose

$$d = -\varepsilon \nabla J(d^\star)$$

where ε is a positive parameter. With this choice, we note that

$$J(D) = J(d^\star + d) \approx J(d^\star) - \varepsilon \nabla J(d^\star) \cdot \nabla J(d^\star) < J(d^\star)$$

and we therefore expect $D = d^\star + d$ to be a better drug than $d^\star$ if ε is small.

The effect of this procedure is illustrated in Figure 16. We show the open probability density functions of the wild type channel, the mutant channel and the mutant channel treated with improved versions of lidocaine and mexiteline. All rates are given in Table 5. We note that the improved versions of lidocaine and mexiteline work significantly better than the originals. Note that suggested improvements are very specific; e.g. for lidocaine we suggest that the rate d_3 is kept as it is and that the rate d_4 is reduced by a factor of 4. Similarly, for mexiteline, the rate d_1 should be kept as it is, but the rate d_2 should be reduced as much as possible. However, we do not know if it possible to construct drugs with these properties.

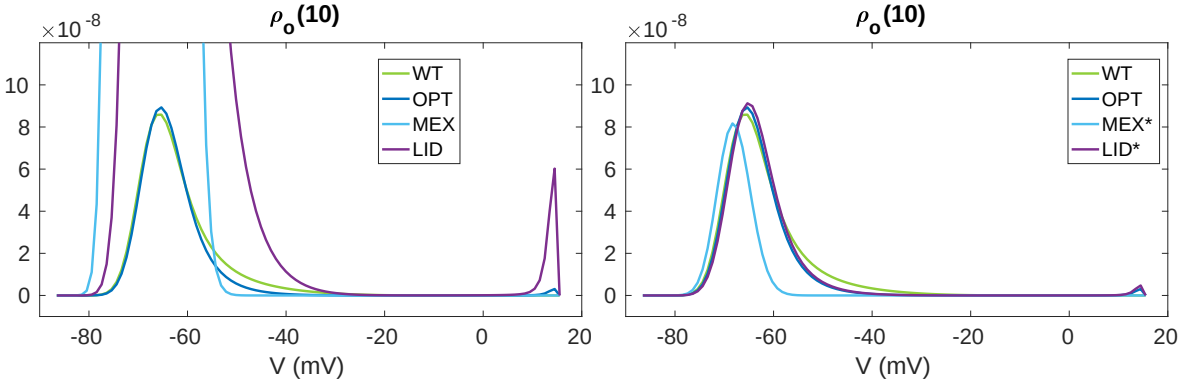

Figure 16: Improving existing drugs Right: The improved versions of lidocaine and mexiteline work well and are much improved from the original; the rates applied are given in Table 5.

4 Conclusion

In summary, we have reviewed the development of mathematical methods for analyzing single channel flow of ions using Markov models in conjunction with stochastic differential equations. The Markov models are ideally suited to represent both the wild type channel, channels that are affected by a mutation and the effect of a drug on a mutant channel. Deterministic PDEs describing the PDFs of the states of the Markov model were introduced, as were the numerical and analytical techniques needed to study these. We have shown how the PDFs can be used to derive optimal theoretical drugs that can completely repair the effect of a mutation and restore function to that of the wild type channel in the case of mutations affecting both internal calcium release and sodium kinetics at the membrane in models of cardiomyocytes. We also discuss how theoretical methods of this type may be related to existing therapies in future work. Finally, we would like to reiterate that our results are theoretical indications of what properties would be favorable for drugs, but we do not know if drugs with these properties can actually be produced.

References

[1] Bertil Hille. *Ion Channels of Excitable Membranes*, volume 507. Sinauer Sunderland, MA, 2001.

[2] Erwin Neher and Bert Sakmann. Single-channel currents recorded from membrane of denervated frog muscle fibres. *Nature*, 260:799–802, 1976.

[3] Bert Sakmann and Erwin Neher. Patch clamp techniques for studying ionic channels in excitable membranes. *Annual Review of Physiology*, 46(1):455–472, 1984.

[4] Bert Sakmann and Erwin Neher, editors. *Single-Channel Recording*. Springer, 1995.

[5] Erwin Neher and Bert Sakmann. Single-channel currents recorded from membrane of denervated frog muscle fibres. *A century of Nature: twenty-one discoveries that changed science and the world*, page 224, 2010.

[6] David Colquhoun and Alan G. Hawkes. Relaxation and fluctuations of membrane currents that flow through drug-operated channels. *Proceedings of the Royal Society of London B: Biological Sciences*, 199(1135):23–262, 1977.

[7] David Colquhoun and Alan G. Hawkes. On the stochastic properties of bursts of single ion channel openings and of clusters of bursts. *Philosophical Transactions of the Royal Society B: Biological Sciences*, 300:1–59, 1982.

[8] Christopher Nicolai and Frederick Sachs. Solving ion channel kinetics with the QuB software. *Biophysical Reviews and Letters*, 8(03n04):191–211, 2013.

[9] FG Ball and SS Davies. Statistical inference for a two-state markov model of a single ion channel, incorporating time interval omission. *Journal of the Royal Statistical Society. Series B (Methodological)*, pages 269–287, 1995.

[10] Rafael A Rosales. Mcmc for hidden markov models incorporating aggregation of states and filtering. *Bulletin of mathematical biology*, 66(5):1173–1199, 2004.

[11] Elan Gin, Martin Falcke, Larry E. Wagner, David I. Yule, and James Sneyd. Markov chain Monte Carlo fitting of single-channel data from inositol trisphosphate receptors. *Journal of Theoretical Biology*, 257(3):460–474, 2009.

[12] Ivo Siekmann, Larry E. Wagner II, David Yule, Colin Fox, David Bryant, Edmund J. Crampin, and James Sneyd. MCMC Estimation of Markov models for ion channels. *Biophysical Journal*, 100(8):1919–1929, 2011.

[13] Ivo Siekmann, James Sneyd, and Edmund J. Crampin. MCMC can detect nonidentifiable models. *Biophysical Journal*, 103(11):2275–2286, 2012.

[14] Keegan E Hines, Thomas R Middendorf, and Richard W Aldrich. Determination of parameter identifiability in nonlinear biophysical models: A bayesian approach. *The Journal of general physiology*, 143(3):401–416, 2014.

[15] Aslak Tveito, Glenn T. Lines, Andrew G. Edwards, and Andrew McCulloch. Computing rates of markov models of voltage-gated ion channels by inverting partial differential equations governing the probability density functions of the conducting and non-conducting states. *Mathematical Biosciences*, 277:126 – 135, 2016.

[16] Colleen E. Clancy and Yoram Rudy. Linking a genetic defect to its cellular phenotype in a cardiac arrhythmia. *Nature*, 400:566–569, 1999.

[17] Colleen E. Clancy and Yoram Rudy. Na^+ channel mutation that causes both Brugada and long-QT syndrome phenotypes: A simulation study of mechanism. *Circulation*, 105(10):1208–1213, 2002.

[18] G Faber and Y Rudy. Calsequestrin mutation and catecholaminergic polymorphic ventricular tachycardia: A simulation study of cellular mechanism. *Cardiovascular Research*, 75(1):79–88, July 2007.

[19] Zheng I. Zhu and Colleen E. Clancy. L-type Ca^{2+} channel mutations and T-wave alternans: a model study. *AJP: Heart and Circulatory Physiology*, 293(6):H3480–H3489, October 2007.

[20] A Tveito and GT Lines. *Computing Characterizations of Drugs for Ion Channels an d Receptors Using Markov Models*. Springer International Publishing, Lecture Notes, Vol. 111, 279 pages. Open access, 2016.

[21] Luc M. Hondeghem and Bertram G. Katzung. Time- and voltage-dependent interactions of antiarrhythmic drugs with cardiac sodium channels. *Biochimica et Biophysica Acta*, 472(3-4):373–398, 1977.

[22] L. M. Hondeghem and B. G. Katzung. Antiarrhythmic agents: the modulated receptor mechanism of action of sodium and calcium channel-blocking drugs. *Annual Review of Pharmacology and Toxicology*, 24:387 – 423, 1984.

[23] Colleen E. Clancy, Zheng I. Zhu, and Yoram Rudy. Pharmacogenetics and anti-arrhythmic drug therapy: A theoretical investigation. *AJP: Heart and Circulatory Physiology*, 292(1):H66–H75, 2007.

[24] Jonathan D Moreno, Z Iris Zhu, Pei-Chi Yang, John R Bankston, Mao-Tsuen Jeng, Chaoyi Kang, Lianguo Wang, Jason D Bayer, David J Christini, Natalia A Trayanova, et al. A computational model to predict the effects of class I anti-arrhythmic drugs on ventricular rhythms. *Science Translational Medicine*, 3(98):98ra83, 2011.

[25] Lucia Romero, Beatriz Trenor, Pei-Chi Yang, Javier Saiz, and Colleen E. Clancy. In silico screening of the impact of hERG channel kinetic abnormalities on channel block and susceptibility to acquired long QT syndrome. *Journal of Molecular and Cellular Cardiology*, 72:126–137, July 2014.

[26] Jonathan D Moreno, Timothy J Lewis, and Colleen E Clancy. Parameterization for in-silico modeling of ion channel interactions with drugs. *PloS one*, 11(3):e0150761, 2016.

[27] Duane Q. Nykamp and Daniel Tranchina. A population density approach that facilitates large-scale modeling of neural networks: Analysis and an application to orientation tuning. *Journal of Computational Neuroscience*, 8(1):19–50, 2000.

[28] Gregory D. Smith. Modeling the stochastic gating of ion channels. In C. P. Fall, E. S. Marland, J. M. Wagner, and J. J. Tyson, editors, *Computational Cell Biology*, volume 20 of *Interdisciplinary Applied Mathematics*, chapter 11, pages 285–319. Springer,

New York, 2002.

[29] Marco A. Huertas and Gregory D. Smith. The dynamics of luminal depletion and the stochastic gating of Ca^{2+}-activated Ca^{2+} channels and release sites. *Journal of Theoretical Biology*, 246(2):332–354, 2007.

[30] Paul C. Bressloff. *Stochastic Processes in Cell Biology*, volume 41. Interdisciplinary Applied Mathematics, Springer International Publishing, 2014.

[31] Bertil Hille. Local anesthetics: hydrophilic and hydrophobic pathways for the drug-receptor reaction. *Journal of General Physiology*, 69(4):497–515, 1977.

[32] C. Frank Starmer. How antiarrhythmic drugs increase the rate of sudden cardiac death. *International Journal of Bifurcation and Chaos*, 12(9):1953–1968, 2002.

[33] Aslak Tveito, Glenn T. Lines, Pan Li, and Andrew McCulloch. Defining candidate drug characteristics for Long-QT (LQT3) syndrome. *Mathematical Biosciences and Engineering*, 8(3):861–73, 2011.

[34] Borbala Mazzag, Christopher J. Tignanelli, and Gregory D. Smith. The effect of residual Ca^{2+} on the stochastic gating of Ca^{2+}-regulated Ca^{2+} channel models. *Journal of Theoretical Biology*, 235(1):121–150, 2005.

[35] George S. B. Williams, Marco A. Huertas, Eric A. Sobie, M. Saleet Jafri, and Gregory D. Smith. A probability density approach to modeling local control of calcium-induced calcium release in cardiac myocytes. *Biophysical Journal*, 92:2311–2328, 2007.

[36] George S. B. Williams, Marco A. Huertas, Eric A. Sobie, M. Saleet Jafri, and Gregory D. Smith. Moment closure for local control models of calcium-induced calcium release in cardiac myocytes. *Biophysical Journal*, 95:1689–1703, 2008.

[37] James Keener and James Sneyd. *Mathematical Physiology: I: Cellular Physiology*. Springer, New York, 2010.

[38] Aslak Tveito and Glenn T. Lines. A note on a method for determining advantageous properties of an anti-arrhythmic drug based on a mathematical model of cardiac cells. *Mathematical Biosciences*, 217(2):167–173, 2009.

[39] Randall J. LeVeque. *Finite Volume Methods for Hyperbolic Problems*. Cambridge Texts in Applied Mathematics, 2002.

[40] H. Joachim Schroll, Glenn T. Lines, and Aslak Tveito. On the accuracy of operator splitting for the monodomain model of electrophysiology. *International Journal of Computer Mathematics*, 84(6):871–885, 2007.

[41] Joakim Sundnes, Glenn Terje Lines, and Aslak Tveito. An operator splitting method for solving the bidomain equations coupled to a volume conductor model for the torso. *Mathematical Biosciences*, 194(2):233–248, 2005.

[42] Peter Deuflhard and Folkmar Bornemann. *Scientific computing with ordinary differential equations*, volume 42. Springer Science & Business Media, 2012.

[43] Aslak Tveito, Hans Petter Langtangen, Bjørn Frederik Nielsen, and Xing Cai. *Elements of Scientific Computing*, volume 7. Springer-Verlag, Berlin Heidelberg, 2010.

[44] MB Cannell, CHT Kong, MS Imtiaz, and DR Laver. Control of sarcoplasmic reticulum ca 2+ release by stochastic ryr gating within a 3d model of the cardiac dyad and importance of induction decay for cicr termination. *Biophysical journal*, 104(10):2149–2159, 2013.

[45] Yan-Ting Zhao, Carmen R Valdivia, Georgina B Gurrola, Patricia P Powers, B Cicero Willis, Richard L Moss, José Jalife, and Héctor H Valdivia. Arrhythmogenesis in a catecholaminergic polymorphic ventricular tachycardia mutation that depresses ryanodine receptor function. *Proceedings of the National Academy of Sciences*, 112(13):E1669–E1677, 2015.

[46] M.A. Walker, G.S.B. Williams, T. Kohl, S.E. Lehnart, M. Saleet Jafri, J.L. Greenstein, W.J. Lederer, and R.L. Winslow. Superresolution modeling of calcium release in the heart. *Biophys J.*, 107(12):3018–3029, 2014.

[47] C.E. Clancy, Z.I. Zhu, and Y. Rudy. Pharmacogenetics and anti-arrhythmic drug therapy: a theoretical investigation. *Am J Physiol Heart Circ Physiol*, 292(1):H66–75, 2007.

[48] P.B. Bennett, K. Yazawa, N. Makita, and Jr A.L. George. Molecular mechanism for an inherited cardiac arrhythmia. *Nature*, 376:683–685, 1995.

[49] Rashmi Chandra, C. Frank Starmer, and Augustus O. Grant. Multiple effects of KPQ deletion mutation on gating of human cardiac Na^+ channels expressed in mammalian cells. *AJP: Heart and Circulatory Physiology*, 274(5):H1643–H1654, 1998.

[50] Aslak Tveito, Glenn Terje Lines, Ola Skavhaug, and Mary M. Maleckar. Unstable eigenmodes as possible drivers for cardiac arrhythmias. *Journal of the Royal Society Interface*, 8(61):1212–1216, 2011.

[51] L. M. Livshitz and Y. Rudy. Regulation of Ca2+ and electrical alternans in cardiac myocytes: role of CAMKII and repolarizing currents. *Am J Physiol Heart Circ Physiol*, 292(6):H2854–2866, 2007.